Clinical issues regarding misclassification by Dixon based PET/MR attenuation correction

Eunjung Kong MD,
Ihnho Cho MD

Department of Nuclear Medicine, College of Medicine, Yeungnam University, Daegu, Republic of Korea

Keywords: PET - MRI
- Multimodal imaging
- Artifacts
- Attenuation correction

Correspondence address:
Ihn Ho Cho,
317-1 Daemyeong 5-dong,
Nam-gu, Daegu 705-717,Korea
Tel: +82-53-620-3074,
Fax: +82-53-620-3079
ihcho@med.yu.ac.kr

Received:
19 February 2015
Accepted revised:
10 March 2015

Abstract

Objective: The Dixon sequence is acquired for attenuation correction (AC) of positron emission tomography (PET) data in integrated PET/magnetic resonance (MR). However it sometimes misclassifies soft tissue and fat in μ-map. In the present study, we investigated factors related to this misclassification and their clinical impacts. **Subject and methods**: Forty-eight oncological patients (19 males and 29 females, mean age: 59±11 years old) underwent a single fluorine-18 fluorodeoxyglucose (^{18}F-FDG) injection/dual-imaging protocol on PET/computed tomography (CT) and subsequently PET/MR. Patients were assigned to either of two groups; group A with a misclassification in at least one bed position or group B with a correctly classified μ-map. We compared body mass index (BMI), lean body mass, fasting duration, volume of hydration and age between group A and group B. In addition, we analyzed the impact of PET quantification using standard uptake ratio (SUR) defined as uptake in volume of interest/uptake in thigh muscle. The Dixon-AC SUR was compared with CT-AC SUR in misclassified bed positions and correctly classified bed positions. All patients were scanned in four bed positions by PET/MR. Ten patients were assigned to group A; six showed misclassification in a bed position (5 in head and 1 in abdomen), three patients in 3 bed positions (head-thorax-abdomen), and one patient in partial bed position in neck. **Results**: Misclassification was observed in 21% of 48 patients. Group A and group B showed no statistically significant differences in BMI, lean body mass, fasting duration or age, however the volume of hydration in group A (245mL) was smaller than in group B (452.6mL) (P=0.027). In group A, we analyzed Dixon-AC SUR/CT-AC SUR ratios in 16 misclassified and 24 correctly classified regions, and ratios in these regions were significant different 0.80 and 0.93, respectively (P=0.046). **Conclusion**: Because no corrective method has been devised after a scan, we recommend that Dixon images with μ-maps should be checked before interpreting PET/MR images and emphasize the importance of hydration, pre-examination. Misclassification errors do not change the presence of ^{18}F-FDG uptake but can have significant impacts on PET quantification in affected bed positions.

Hell J Nucl Med 2015; 18(1): 42-47 *Published online: 31 March 2015*

Introduction

Recently, hybrid positron emission tomography (PET)/magnetic resonance (MR) system has become a reality, and is being transformed from research prototypes to clinical systems [1]. Hybrid PET/MR system provides complementary multimodal information about metabolism, receptor status, perfusion, diffusion and tissue characterization, together with high soft tissue contrast as compared with computed tomography (CT), and without additional radiation exposure [2, 3]. Although the preliminary clinical results obtained using hybrid PET/MR systems are promising [4-6], attenuation correction (AC) is still a major drawback [7-9]. Because MR is not able to calculate the electron densities of objects, PET/MR uses an indirect way to compute an attenuation map (μ-map). Several approaches have been proposed to cope with this problem, and segmentation based on the 2-point Dixon algorithm offers a promising solution [10]. This straightforward approach divides the body into four tissue classes (air, lung, soft tissue, fat), and has been shown to provide PET image results comparable to those obtained by standard CT based reconstruction [11]. Dixon is a common sequence for water and fat segmentation in standalone MRI, and a single acquisition results in four image series (in-phase, opposed-phase, water, and fat contrast), which are used to compute μ-map. The Dixon-AC technique has been widely used in clinical setting, but sometimes we have experienced misclassification errors because soft tissue was interpreted as fat in some bed positions. It has been established that Dixon sequence is prone to water/ fat swapping artifact, for example fat being assigned to brain instead of soft tissue.

In this work, we investigated the incidence of μ-map misclassification errors, relating

factors, and their impact to PET quantification. Positron emission tomography images with CT-AC were used as reference for comparison of the PET quantification.

Materials and methods

PET/CT and PET/MR data acquisition

The study population comprised of 48 consecutive patients (19 men and 29 women), mean age±SD=59±11 years), in whom fluorine-18 fluorodeoxyglucose PET/CT (^{18}F-FDG PET/CT) was performed for staging or follow-up of a malignant disorder. The patients that provided informed consent and were able to undergo another scan after a PET/CT examination were selected from July 2012 to August 2012. This study was approved by the Institutional Review Board of our institute.

All subjects underwent a single ^{18}F-FDG injection of 398±71MBq and a dual-imaging protocol with PET/CT and subsequently with PET/MR. All patients fasted for at least 6h before ^{18}F-FDG administration and blood glucose concentration was confirmed to be less than 150mg/dL. Fluorine-18-FDG PET/CT scans were performed on a Discovery ST or VCT scanner (GE Healthcare, Milwaukee, WI, USA). After a localization scout scan, a CT scan (120kVp, 120mA) was performed for AC. Data from PET acquisition started 86±18min post-injection with 3min per bed position. Subsequently, integrated PET/MR (BiographmMR, Siemens Medical Solutions, Erlangen, Germany) was performed (131±25min after ^{18}F-FDG injection) using an approved surface coil for PET/MR that improves image quality and reduces MR imaging time. First, a localizer MR scan was performed to define bed positions and then PET and MR for AC were started at the same bed position simultaneously. The PET scan was obtained over 2 min, and a coronal 2-point Dixon 3D volumetric interpolated breath-hold examination (VIBE) T1-weighted MR sequence was acquired to generate the μ-map over 19s. Coronal T1-weighted turbo spin echo and axial T2-weighted fat saturated half-Fourier single-shot turbo spin-echo (HASTE) sequences were then obtained during PET acquisition.

A 3D ordered-subsets expectation maximization (3D OSEM) iterative reconstruction algorithm was applied with two iterations and 28 subsets for PET/CT PET data, and with two iterations and 21 subsets for PET/MR PET data. A 128×128 matrix was used for PET/CT, and a 172×172 matrix for PET/MR and both PET data sets were filtered with a 6mm full width at half maximum.

Data analysis

An experienced nuclear medicine physician reviewed μ-maps to confirm misclassifications using advanced reading software (Syngo.via, Siemens Medical Solutions). Patients were divided into 2 groups, group A μ-maps had soft tissue/fat misclassification and the group B μ-maps were correctly classified (Figure 1). We compared body mass index (BMI), lean body mass, fasting duration, volume of hydration and age in these two patients' groups.

We also examined whether μ-map misclassification could change PET quantification. This analysis was performed on group A patients only. We used volume of interest (VOI)-to-thigh muscle uptake ratio, which we refer to as standard uptake ratio (SUR), because it has been shown that standardized uptake value (SUV) on PET/MR images are significantly smaller than SUV on PET/CT images [11]. A nuclear medicine physician manually drew VOI on regions of normal physiologic uptake and on malignant lesions (Figure 2). Four physiologic regions were used to classify VOI locations; cerebellum, blood pool of the aortic arch, liver, or bone (5th lumbar vertebra). In order to avoid bias caused by multiple lesions, one or two unequivocal malignant lesions per patient were included in the analysis. We treated SUR determined using CT-AC as the gold standard and compared these with SUR obtained after applying Dixon-AC (Figure 2).

All statistical analysis was performed using IBM SPSS version 19.0 (SPSS, Chicago, IL, USA). The Shapiro-Wilk test was used to determine whether variables were normally distributed. The t- test and Mann-Whitney U test were used to compare clinical factors in group A and group B. Spearman's correlation was used to evaluate the relationship between SUR obtained by PET/CT and PET/MR and the paired t-test was used to determine the significance of differences between SUR ratios determined using the two imaging modalities. Statistical significance was accepted for P values <0.05.

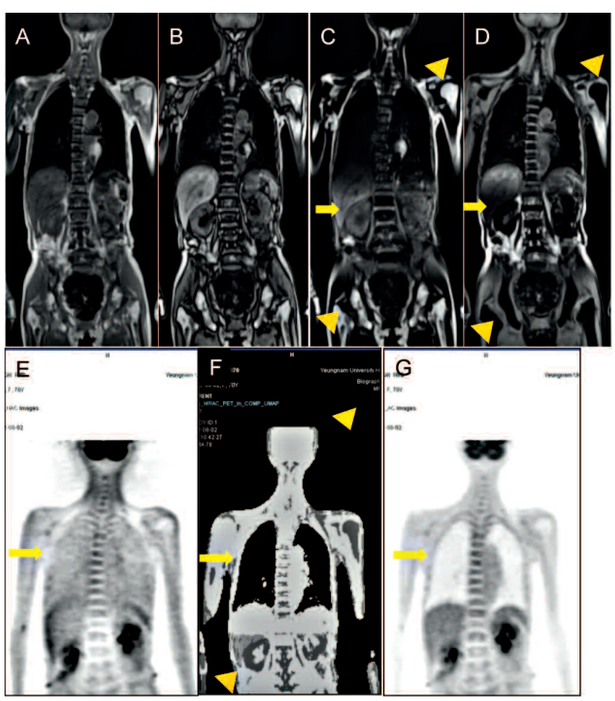

Figure 1. ^{18}F-FDG PET/MR study of a 70 years old woman with stomach cancer. (A) Coronal in-phase image. (B) Coronal opposed-phase image. (C) Coronal fat contrast image with water/fat swapping artifact in abdomen. (D) Coronal water contrast image with water/fat swapping artifact. (E) PET emission image before AC. (F) Dixon-based attenuation map from A-D illustrating misclassification soft tissue to fat in lower liver, kidney, femur and humerus (arrow and arrow head). (G) PET emission image from PET/MR following Dixon-AC using F showing no visual difference between upper and lower liver, despite of misclassification on Dixon-based attenuation map (arrow).

Results

Forty eight patients were included in the study and all underwent both PET/CT and PET/MR. Oncologic diagnosis of the 48 patients included breast cancer (n=10), gastric cancer (n=7), lung cancer (n=5), lymphoma (n=5), thyroid cancer (n=5), esophageal cancer (n=2), hepatocellular carcinoma (n=2), tonsil cancer (n=1), malignant melanoma (n=1), common bile duct cancer (n=1), liposarcoma (n=1), prostate cancer (n=1), and sternal mass (n=1). In 47 of 48 patients soft tissue was classified as fat in femur, and 43 of 46 had the same artifact in their humeri. In addition, misclassifications were found in 10 patients/16 bed positions in other than bone marrow. Six patients had misclassifications in a single bed position (5 head and 1 abdomen), three in 3 bed positions (head-thorax-abdomen), and one patient in partial bed position of neck area. Unexpectedly, an additional erroneous soft tissue segment was visualized outside of abdominal skin in all 48 patients and half of them also showed extra soft tissue segment outside of back skin. After applying of maximum likelihood reconstruction of attenuation and activity (MLAA) the dorsal side artifact was corrected. In addition, a woman showed an erroneous soft tissue segment in the supradiaphragmatic area (Figure 3). To identify relevant factors associated with misclassifications, we compared group A and group B with respect to clinical factors. There were no statistically significant intergroup differences for BMI, lean body mass, fasting duration, or age. However, the volume of hydration was smaller in group A (245mL) than in group B (452.6mL) (P=0.027, Table 1).

To determine the impact of μ-map misclassification on PET quantification, we compared Dixon AC SUR-to-CT AC SUR ratios between misclassified beds and correctly classified bed positions. This analysis included 16 misclassified and 24 correctly classified regions for physiologic uptake. Measured SUR values in PET/CT and PET/MR showed significant correlation for both misclassifications (rho=0.949, P<0.01) and correct classifications (rho=0.804, P<0.01), respectively. However, Dixon AC SUR-to-CT AC SUR was lower in misclassification (0.80) than in correct classification (0.93 (P=0.046 Table 2). To confirm the impact of PET quantification on the malignant lesions, we analyzed 5 malignant lesions in 3 patients in misclassified beds and another 5 malignant lesions in 3 patients in correctly classified bed positions. No difference was found between misclassified (0.85) and correctly classified (0.83) lesions (P>0.05, Table 3). Average underestimation of SUR in Dixon-AC PET with misclassification μ-map versus correct μ-map across all physiologic regional uptake was 16%, but malignant lesion uptake did not make significant change.

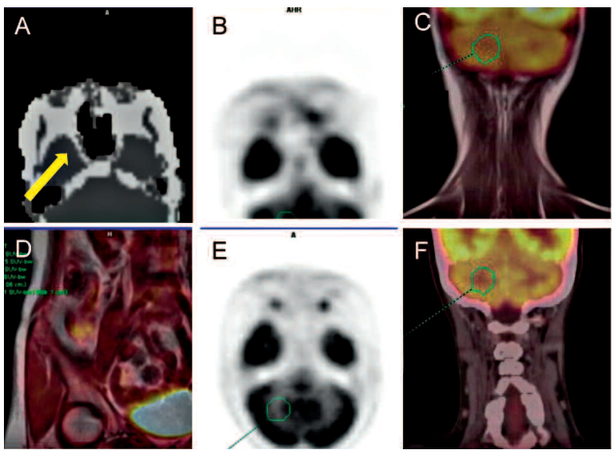

Figure 2. ^{18}F-FDG PET/MR study of a 47 years old woman with breast cancer. (A) Misclassification error in brain in the attenuation map. (B, C) volume of interest (VOI) in right cerebellum for physiologic regional uptake in PET and PET/MR following Dixon-AC; SUVmean=3.82, SUR=5.38 (3.81/0.71). (D) VOI in right thigh muscle for reference; SUVmean=0.71. (E,F) VOI in right cerebellum in PET and PET/CT following CT-AC; SUVmean=5.86, SUVmean of right thigh 0.92 (figure is not included), SUR=6.37 (5.86/0.92).

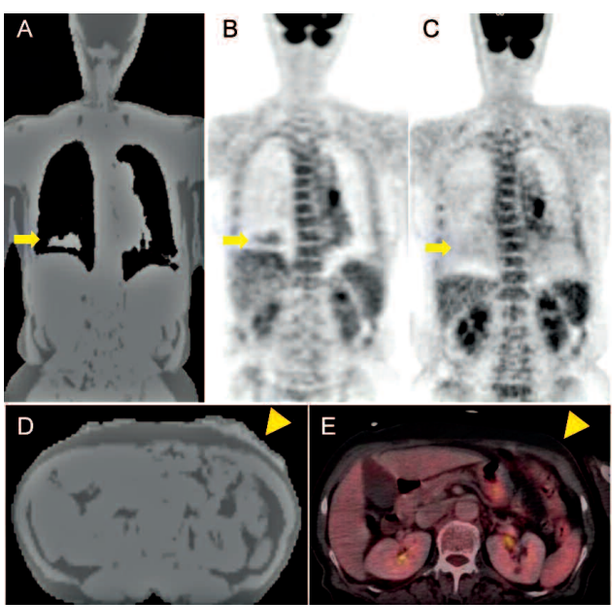

Figure 3. ^{18}F-FDG PET/MR study of a 73 years old woman with thyroid cancer. (A) Dixon-based attenuation map depicting erroneous soft tissue segment in supradiaphragmatic area. (B) PET emission image from PET/MR following Dixon-AC using A showing area of false positive uptake. (C) PET emission image from PET/CT following CT-AC showing no abnormal radio- activity. (D) Dixon-based attenuation map depicting erroneous soft tissue segment outside of abdominal skin. (E) PET/CT image corresponding to D showing nothing in there.

***Table 1**. Comparison of clinical factors between Group A and Group B*

	Group A (soft tissue/fat misclassification in μ-map	Group B (Correctly classified μ-map)	Difference
Numbers of patients	10	38	
Age	62.1±12.5	58.6±10.6	NS
BMI (kg/h^2)	21.52±4.4	22.85±2.8	»
Lean body mass	41.16±5.5	42.16±6.9	»
Fasting duration (h)	10.6 ±4.4	11.1 ±5.5	»
Volume of hydration (mL)	245±125.7	452.6±315.1	P=0.027

NS: No significant difference

***Table 2**. Impact on PET quantification in physiologic regional uptake*

	Misclassified bed position	Correctly classified bed position	Difference
Number and locations of regions	16 (8 cerebellum, 3 BPA, 4 liver and 1 thyroid)	24 (2 cerebellum, 7 BPA, 5 liver and 10 5th lumbar vertebra)	
Dixon AC SUVmean	2.2±1.3	1.3 ±0.8	
CT AC SUVmean	3.1±1.9	1.7 ±1.1	
Dixon AC SUR	4.7±2.8	2.6 ±1.5	
CT AC SUR	6.0±4.0	2.9 ±1.8	
SUR ratio	0.8±0.12	0.93±0.22	P=0.046

BP: blood pool of aortic arch; SUR=SUVmean/SUVmean of thigh; SURratio=Dixon AC SUR/CT AC SUR

***Table 3**. Impact on PET quantification in malignant lesions uptake*

	Misclassified bed position	Correctly classified bed position	Difference
Number and locations ofmalignant lesions	5 (metastatic lung mass, thyroid cancer, stomach cancer, metastatic mediastinal and abdominal lymphadenopathy)	5 (hepatic metastasis, lung cancer, metastatic mediastinallymphoadenopathy, bone metastasis, and pericardial mass)	
Dixon AC SUVmax	9.2± 4.3	9.1± 2.6	NS
CT AC SUVmax	12.1± 6.6	12.5± 4.1	»
Dixon AC SUR	21.7± 9.8	18.7± 8.1	»
CT AC SUR	25.9±11.5	23.2±11.2	»
SUR ratio	0.85±0.2	0.83±0.1	»

NS: No significant difference; SUR=SUVmax/SUVmean of thigh; SURratio=Dixon AC SUR/CT AC SUR

Discussion

Dixon sequence has limitations, in particular, an artifact occasionally occurs when the computations converge to the wrong substance, to produce a fat-only image when a water-only image is desired. This so-called "water-fat swap" is the cause of misclassification error on μ-map. In the present study, we found that the incidence of misclassification between soft tissue and fat was 21% by patient and 8.3% by bed position analysis. The most commonly affected bed position was head and neck, which accounted for 50% of misclassification. Because no software is currently available to correct for misclassification errors after PET/MR acquisition, and currently, there is no way of preventing such misclassification, one must verify Dixon images with μ-map before reading PET/MR images.

In the present study, the femurs of 47 patients and humeri of 43 patients were misclassified as fat, because bone was replaced by fat tissue due to a partial volume effect in bone marrow. Cortical bone, which shows nearly no MR signal despite having high attenuating power was assigned to soft tissue in the use of a 4 classes segmented μ-map [11]. Under-correction of bone attenuation is well known, the misclassification errors made worse underestimation for bone AC [11], probably because the coefficient of fat ($0.0854cm^{-1}$) was smaller than that of soft tissue ($0.100cm^{-1}$) in 4 classes segmented μ-map. In the present study, we found that poor hydration was related to misclassification. Thirty-five percent of patients with volume of hydration ≤200mL exhibited misclassification errors, but only 11% of patients with >200mL showed errors. Furthermore, only 6% of patients with >500mL volume of hydration showed errors. On the other hand, BMI, lean body mass, fasting duration and age, did not show any significant impact on misclassification error. An unexpected error was that a soft tissue segment in the lung was a respiratory motion related artifact as shown in PET/CT. As occurs in PET/CT scans, subject motion can disrupt μ-map and this effect should be carefully considered. In addition, misclassification error was not only an entire bed position artifact, but it could also occur in only part of the image. Nevertheless, in a patient homogeneity of the B0 magnetic field was thought to be the cause of partial bed misclassification on the neck area.

In a clinical setting, PET is used to detect tumors or tumor metastasis. Quantitative PET information enables us to evaluate the response to cancer therapy [12], and has been demonstrated for both chemotherapy and radiotherapy [13, 14]. So, we evaluated the accuracy of PET quantifications of the normal physiologic uptake and of the malignant lesion uptake in misclassification on μ-map. Misclassification errors could make significant decrease in quantification of the regional physiologic uptake. Misclassification that assumed the soft tissue to be fat has resulted in noticeable local SUR differences. For instance, the local SUR of cerebellum is 5.4 by Dixon AC PET, and 6.4 by CT-AC PET (Figure 2). Overall, the relative under-correction for Dixon-AC SUR/CT-AC SUR in VOI defined in normal physiologic uptake is 0.8 in misclassification and 0.93 in correct classification. It can be deduced that attenuation coefficient differences could cause under-correction in areas of misclassification. Although, misclassification generates a lower systematic negative bias of tracer uptake in our study, the visual PET image was not enough to guess the misclassification errors (Figure 1). Despite the bias induced by misclassification, our data are in accord with recently published results which showed that MR-AC underestimated ^{18}F-FDG uptake in quantitative analysis than CT-AC but, showed good correlation with CT-AC [11, 15]. High Spearman's correlation coefficients indicate a statistically significant relationship

between Dixon-AC SUR and CT-AC SUR.

We also analyzed five malignant lesions in misclassified and correctly classified bed positions respectively. Only one lesion-a metastatic lung mass in a misclassified bed-showed higher uptake by PET/MR (SUR 6.7) than by PET/CT (SUR 5.7). The remaining 9 lesions showed lower uptake by PET/MR. Dixon-AC SUR/CT-AC SUR ratio varied from 0.64 to 1.14 in misclassified beds and from 0.73 to 0.98 in correctly classified beds. Unfortunately, in the present study the number of malignant lesions was too small to reach a conclusion; misclassification could not have an impact in PET quantification in malignant lesions. In malignancy ^{18}F-FDG uptake is much more complex than in physiologic uptake. Furthermore, ^{18}F-FDG uptake in malignancy is affected by a variety of cell-biological factors and shows interin dividual variability [16].

Although, segmentation accuracy is an important issue for segmentation-based PET/MR-AC approaches, few studies have been conducted on the accuracy of segmentation [7-9, 17]. Brendle et al (2015) [7] recently presented several types of artifacts in segmentation based μ-maps, and showed artifacts that cause significant SUV changes in areas erroneously assigned to be air instead of soft tissue (eg, metal artifacts) and to be soft tissue instead of lung. Nevertheless, they found that diagnoses were not changed by μ -map artifacts. However, their results did not show differences in SUV between misclassifications and correct classifications. Differences between their findings and ours are probably due to different subject groups, gold standards, and quantification factors. Furthermore, both studies were conducted using relatively small cohorts, and thus, we recommend further work to be conducted on larger numbers of subjects. Another study by Ladefoged et al (2014) [9] described the impact of tissue misclassification by soft tissue-fat inversion in PET/MR for brain or head and neck images. The researchers also found that tissue inversion of soft tissue and fat had relatively high prevalence (8.1%) and could induce a large quantitative effect of up to 35%. An interesting finding of them, which was the error effect of misclassification was larger in the center area than in the periphery. Our results agree with those of Ladefoged et al [9] in terms of the serious effect by misclassification, but the above researchers dealt only with brain or head and neck areas.

The strong point of our study was that we studied actual patients' data obtained during clinical practice and also that their practical use in higher misclassification errors were related with a smaller volume of pre-examination hydration.

This study has several limitations. First, the number of enrolled patients was small and the study was performed in a retrospective manner at a single institute. Second, PET/CT and PET/MR scans were not obtained at the same time, which could have caused intra-individual variations in organ systems and in tracer kinetics. In addition, different AC methodologies result in different PET quantification in PET/CT and PET/MR, and these require further clarification. Furthermore, we did not address metal-induced artifacts, truncation artifacts, field of view edge artifacts, or other.

Although, it is expected that segmentation methods for μ-map creation will provide improvements, it should be borne in mind that MR-AC with the Dixon procedure could cause artifacts that interfere with PET quantification. Therefore, we strongly recommend Dixon images with μ-maps be checked as part of the reading procedure for artifacts and emphasize the importance of hydration pre-examination.

In conclusion, hybrid PET/MR raises expectations that it will prove to be a novel, powerful multimodality imaging tool. The present study contributes to the development of design of hybrid PET/MR, and also can be considered as a helpful tool in daily clinical practice.

Acknowledgements

This research was supported by Yeungnam University research grants (2012).

The authors declare that they have no conflicts of interest.

Bibliography

1. Pichler BJ, Kolb A, Nagele T, Schlemmer HP. PET/MRI: paving the way for the next generation of clinical multimodality imaging applications. *J Nucl Med* 2010; 51: 333-6.
2. Hirsch FW, Sattler B, Sorge I et al. PET/MR in children. Initial clinical experience in paediatric oncology using an integrated PET/MR scanner. *Pediatr Radiol* 2013; 43: 860-75.
3. Zukotynski KA, Fahey FH, Kocak M et al. Evaluation of ^{18}F-FDG PET and MRI associations in pediatric diffuse intrinsic brain stem glioma: a report from the Pediatric Brain Tumor Consortium. *J Nucl Med* 2011; 52: 188-95.
4. Kong EJ, Chun KA, Bom HS et al. Initial experience of integrated PET/MR mammography in patients with invasive ductal carcinoma. *Hell J Nucl Med* 2014; 17: 171-6.
5. Wiesmuller M, Quick HH, Navalpakkam B et al. Comparison of lesion detection and quantitation of tracer uptake between PET from a simultaneously acquiring whole-body PET/MR hybrid scanner and PET from PET/CT. *Eur J Nucl Med Mol Imaging* 2013; 40: 12-21.
6. Kong EJ, Lee SH, Cho IH. Myocardial Fibrosis in Hypertrophic Cardiomyopathy Demonstrated by Integrated Cardiac F-18 FDG PET/MR. *Nucl Med Mol Imaging* 2013; 47: 196-200.
7. Brendle C, Schmidt H, Oergel A et al. Segmentation-Based Attenuation Correction in Positron Emission Tomography/Magnetic Resonance: Erroneous Tissue Identification and Its Impact on Positron Emission Tomography Interpretation. *Investigative Radiology* 2015 Jan 12 [Epub ahead of print].
8. Keller SH, Holm S, Hansen AE et al. Image artifacts from MR-based attenuation correction in clinical, whole-body PET/MRI. *Magma* 2013; 26: 173-81.
9. Ladefoged C, Hansen A, Keller S et al. Impact of incorrect tissue classification in Dixon-based MR-AC: fat-water tissue inversion. *EJNMMI Phys* 2014; 1: 1-9.
10. Coombs BD, Szumowski J, Coshow W. Two-point Dixon technique for water-fat signal decomposition with B0 inhomogeneity correction. *Magn Res in Med* 1997; 38: 884-9.
11. Martinez-Moller A, Souvatzoglou M, Delso G et al. Tissue classification as a potential approach for attenuation correction in whole-body PET/MRI: evaluation with PET/CT data. *J Nucl Med* 2009; 50: 520-6.
12. Kostakoglu L, Goldsmith SJ. ^{18}F-FDG PET evaluation of the response to therapy for lymphoma and for breast, lung, and colorectal carcinoma. *J Nucl Med* 2003; 44: 224-39.
13. Chaiken L, Rege S, Hoh C et al. Positron emission tomography with fluorodeoxyglucose to evaluate tumor response and control after radiation therapy. *Inter J Rad Oncol, Biology, Physics* 1993; 27: 455-64.
14. Young H, Baum R, Cremerius U et al. Measurement of clinical and subclinical tumour response using [^{18}F]-fluorodeoxyglucose and

positron emission tomography: review and 1999 EORTC recommendations. European Organization for Research and Treatment of Cancer (EORTC) PET Study Group. *Eur J Cancer* 1999; 35: 1773-82.
15. Drzezga A, Souvatzoglou M, Eiber M et al. First clinical experience with integrated whole-body PET/MR: comparison to PET/CT in patients with oncologic diagnoses. *J Nucl Med* 2012; 53: 845-55.
16. Fischman AJ, Alpert NM. FDG-PET in oncology: there's more to it than looking at pictures. *J Nucl Med* 1993; 34: 6-11.
17. Keereman V, Holen RV, Mollet P, Vandenberghe S. The effect of errors in segmented attenuation maps on PET quantification. *Medical Physics* 2011; 38: 6010-9.

Raphael (1483-1520): Transfiguration (1520). Oil in canvas. Vatical Gallery. The last (unfinished) painting of Raphael, who died at the age of 37. At the right down part of this painting one sees the epileptic crisis of a boy whose father begged Christ to help. Notice that both the position of the boy's left hand fingers and the position of his eyes differ from what we usually notice in an epileptic crisis.